Research Article

Study of Effect of Different Shapes of Nanoparticles in Three-Layer Model for Blood Flow in Arterioles

Rekha Bali, Bhawini Prasad*, Swati Mishra

Department of Mathematics, School of Basic & Applied Sciences, Harcourt Butler Technical University, Kanpur-208002, U.P., India
E-mail: jayabhawini@gmail.com

Abstract: Arterioles are pivotal console of hemodynamics as they are significant contributors to pressure. Under various physiological conditions like administration of a drug, arterioles ascertain divergent mechanical forces. The current communication discusses the effect of different shapes of copper nanoparticles inoculated as nano drugs in arterioles. The blood is assumed to be a non-Newtonian fluid and is delineated as nanofluids. The three-layer model is used for modeling the blood flow as it aptly describes the flow of blood in narrow vessels of diameter less than 100 μm. The Hamilton-Crosser model is implemented to describe the thermal conductivity of nanofluid as this model holds in accordance with experimental as well as theoretical results. The expressions are also obtained for density, thermal expansion and viscosity of the considered nanofluid. The equations are solved analytically and graphs have been plotted using MATLAB. The relative consequence of various shapes of nanoparticles like platelets, blades, cylinders and bricks is observed in temperature, velocity and flow rate. It has been investigated through the graphs that brick-shaped nanoparticles have shown a maximum rise in temperature, velocity and flow rate. And reverse results are observed for blade-shaped nanoparticles. The effect of volume fraction, heat source parameter and Grashof number have also been inspected. The considered analysis shows that a suitable shape of nanoparticle can be used to develop the nano drug according to biomedical needs.

Keywords: arterioles, nanoparticles, nanofluids, three-layer model, hamilton-crosser model, heat source parameter

MSC: 92F08, 76Z10, 35D00

Nomenclature

r'	Dimensional radial direction
θ'	Dimensional azimuthal direction
z'	Dimensional axial direction
u'	Dimensional radial fluid velocity
v'	Dimensional azimuthal fluid velocity
w'	Dimensional axial fluid velocity
r	Non-Dimensional radial direction

z	Non-Dimensional axial direction
L	Length of the arteriole
R_0	Radius of the arteriole
R_1'	Dimensional radius of the central region
R_1	Non-Dimensional radius of the central region
R_c	Radius of the core region
P'	Dimensional pressure
P	Non-Dimensional pressure
μ_f	Viscosity of blood
u_{nf}	Viscosity of nanofluid
u_0'	Dimensional velocity of blood in the peripheral layer
u_0	Non-Dimensional velocity of blood in the peripheral layer
u_1'	Dimensional velocity of blood in the central region
u_1	Non-Dimensional velocity of blood in the central region
u_c'	Dimensional velocity of blood in the core region
u_c	Non-Dimensional velocity of blood in the core region
τ_f	Shear stress of blood
τ_{nf}	Shear stress of nanofluid
T'	Dimensional temperature of blood in arteriole
T_0	Temperature of the peripheral layer
T_1	Temperature of the core region
H	Constant heat generation or absorption parameter
k_{nf}	Thermal conductivity of nanofluid
k_f	Thermal conductivity of blood
k_p	Thermal conductivity of nanoparticle
ρ_{nf}	Density of nanofluid
ρ_f	Density of blood
ρ_p	Density of nanoparticle
γ_{nf}	Thermal expansion of nanofluid
γ_f	Thermal expansion of blood
γ_p	Thermal expansion of nanoparticle
g	Acceleration due to gravity
n	Shape factor
ψ	Sphericity
ϕ	Volume Fraction
α	Shape of nanoparticle parameter
u_{avg}	Average velocity of nanofluid
θ	Non-Dimensional temperature
Gr	Grashof Number
β	Heat source parameter
Re	Reynolds Number
Q_0	Volumetric flow rate in peripheral layer
Q_1	Volumetric flow rate in central region
Q_c	Volumetric flow rate in core region
C_p	Specific heat capacity
$F_{r'}$	Body forces in radial direction
$F_{\theta'}$	Body forces in azimuthal direction
$F_{z'}$	Body forces in axial direction
D_{nf}	Thermal diffusivity

1. Introduction

Arterioles are the smallest branch of an artery that conduct blood away from the heart. Arterioles offer 80% impedance to the blood vessels while they transmit blood flow into capillary beds. Thus, they are instrumental in the upstream perfusion pressure for all body parts. Arterioles have a distinctive attribute of their active reciprocation to physical stimuli or alterations in the chemical conditions, in contrast to other blood vessels. The arterioles can be influenced by a disorder called arteriosclerosis that leads to deposition in their vascular wall. This affliction occurs in the patient's renal vasculature with malignant hypertension.

Blood is a heterogeneous fluid consisting of cells suspended in plasma. The prevalence of yield stress and shear thinning action of blood assorts it in the grade of non-Newtonian fluid. The blood in vessels of diameter about 100 μm, shows aberrant rheological effects like the Fahraeus effect and Fahraeus-Lindquist effect, the presence of cell-free layer at the wall and a blunt velocity profile [1-3]. Fahraeus effect and Fahraeus-Lindquist effect are estimated quantitatively. For determining velocity and concentration in a narrow vessel of diameters above 100 μm, like arterioles, researchers depend on the theoretical models devised by examining various cross section boluses. The three-layer model for blood flow provides a pragmatic model for arterioles, comprising of a cell-free layer at the wall constituting of plasma partitioned from the uniform core of red blood cells by the central layer embracing of cells and plasma [1]. This model more suitably fits experimental concentration profiles. The disposition of the wall layer where the red blood cells cannot probe into, has a hematocrit value very close to zero, 7 and it notably rises as one red blood cells radius from the wall [1]. Thus, divaricating the hematocrit values reports more positively for the peripheral layer or red blood cell migration.

Gupta et al. [1] devised a three-layer mathematical model for the blood flow and particle suspensions in tubes of diameter less than 100 μm. They considered a narrow cell-free layer near the wall, a cell-free layer as an intermediate layer and a central core region of evenly spread cell-concentration. Chaturani and Biswas [4] examined the three-layer model for Couette flow of blood. Bali et al. [5] considered the three-layer model for small blood vessels. Debnath et al. [6] analyzed the unsteady dispersion of solute in fluid resembling the properties of blood flowing through a rigid artery using the three-layer model. Roy and Shaw [7] examined the dispersion of a solute in a micro vessel for nanoparticle-based drug delivery. They considered blood as a Casson fluid in the intermediate region.

The novel concept of nanotechnology was put forward by physicist Richard P. Feynmann who was a Nobel prize winner [8]. Since then, nanotechnology is a newfangled concept that needs wide exploration. Owing to the benefits of this pioneering technology, nanoparticles evolved, which are defined as particles with dimensions of at least one nanoscale. Researchers are working greatly toward using nanoparticles for the curing of cardiovascular diseases [9]. Nanoparticles offer a robust mechanism in therapeutics of cardiovascular diseases due to their capability of interacting with the cellular processes and influencing their functions. Pharmaceutical nanotechnology offers sustained and controlled delivery systems [9].

Several researchers have been working in the discipline of nanoparticle-based drug delivery. When the nanoparticles are dispersed in the blood, the blood carries itself as a non-Newtonian fluid. The characteristics of this fluid are described by nanofluids [10]. Nanofluids were introduced by Choi and Eastman [11]. The nanofluids are defined as nanoparticles (like Al, Cu, Ag, Au, Fe, Al_2O_3, CuO, TiO_2, carbon nanotubes, etc.) dispersed in a base fluid [12]. Nanoparticles are present in 2%-5% volume fraction in nanofluids. Here, the blood has been regarded as base fluid. Recently, a number of researchers have studied nanofluid technology experimentally or theoretically in the presence of heat transfer [13-25].

The experimental results have been interpreted and analyzed by different mechanisms such as nanoparticle Brownian motion, nanoparticle aggregation, the chemistry of the surface and convection. Maxwell gave the classical model for the effective thermal conductivity of nanofluids [26]. This model had considered some limited parameters such as thermal conductivity of the base fluid, thermal conductivity of nanoparticles and particle volume fraction. Hamilton-Crosser model estimates the thermal conductivity of nanofluid taking into consideration the particle shape factor [27]. This model is in good agreement with the available experimental data for nanofluids of different shapes of nanoparticles.

Earlier, the researchers have been considering usually only the spherical shape of nanoparticles. But practically, they have limited applications. Clinical diagnosis and drug delivery have a major usage of non-spherical shaped nanoparticles [28]. Nanoparticles of shapes like cylinder, blade, brick and platelets have enormous utilization in drug

delivery.

The analysis of a three-layer model for blood flow in arterioles for different shapes of nanoparticles is a considerably new notion because the impact of shapes of nanoparticles like platelets, blades, cylinders and bricks has not been observed before. The constant heat generation/absorption parameter has also not been discussed earlier for this type of blood flow phenomenon. Also, in order to develop better nanomedicine, the effect of shape of nanoparticles has a vital role in their delivery in small blood vessels. This would develop new possibilities in the field of nanotechnology for medicine. In consideration of the above facts, an effort has been made in this paper to comprehend the effect of varying shapes of nanoparticles modeling the blood flow using the three-layer model of blood in arterioles. The next section discusses this mathematical formulation. The governing mathematical equations are solved analytically in the solution section. The exact solution for temperature, velocity and flow rate are achieved. The graphs have been plotted using MATLAB discussed in the graphical results and discussions section. The effect of distinct shapes of nanoparticles like a cylinder, blade, brick and platelets on temperature, velocity and flow rate have been investigated through graphs. The major findings of our study are encapsulated in the conclusion section. The results of this work will help to give a greater perception of the efficiency of different shapes of nanoparticles and subsequently give a novel insight into biomedical engineering.

2. Mathematical formulation

Steady and laminar flow of blood is considered in an arteriole of length L and radius R_0. The incompressible flow of blood in the narrow vessel is represented by a three-layer model that consists of a peripheral layer of plasma, the central region of the suspension of nanoparticles in blood and the core region comprising of red blood cells. Copper nanoparticles of different shapes are dispersed in blood. Equation of continuity, Navier-Stokes equation and diffusion equations are used to frame the governing equations [29]. Since the flow is laminar low Reynolds number describes the flow (Figure 1).
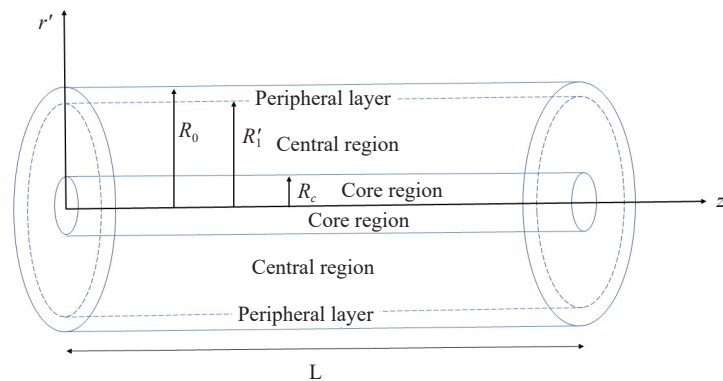
Figure 1. Three-layer model

Equation of continuity in cylindrical co-ordinates:

$$\frac{\partial \rho_{nf}}{\partial t'} = \frac{1}{r'}\frac{\partial (r\rho_{nf}u')}{\partial r'} + \frac{1}{r'}\frac{\partial \rho_{nf}v'}{\partial \theta'} + \frac{\partial \rho_{nf}w'}{\partial z'} = 0 \tag{1}$$

Navier-Stokes equation in cylindrical co-ordinates:

$$\frac{\partial u'}{\partial t'} + u'\frac{\partial u'}{\partial r'} + \frac{v'}{r'}\frac{\partial u'}{\partial \theta'} - \frac{v'^2}{r'} + w'\frac{\partial u'}{\partial z'}$$

$$= F_{r'} - \frac{1}{\rho_{nf}}\frac{\partial p'}{\partial r'} + \frac{\mu_{nf}}{\rho_{nf}}\left(-\frac{u'}{r^2} + \frac{1}{r'}\frac{\partial}{\partial r'}\left(r'\frac{\partial u'}{\partial r'}\right) + \frac{1}{r'^2}\frac{\partial^2 u'}{\partial \theta'^2} + \frac{\partial^2 u'}{\partial z'^2} - \frac{2}{r'^2}\frac{\partial v'}{\partial \theta'}\right) \quad (2)$$

$$\frac{\partial v'}{\partial t'} + u'\frac{\partial v'}{\partial r'} + \frac{v'}{r'}\frac{\partial v'}{\partial \theta'} - \frac{u'v'}{r'} + w'\frac{\partial v'}{\partial z'}$$

$$= F_{\theta'} - \frac{1}{\rho_{nf}}\frac{\partial p'}{\partial \theta'} + \frac{\mu_{nf}}{\rho_{nf}}\left(-\frac{v'}{r^2} + \frac{1}{r'}\frac{\partial}{\partial r'}\left(r'\frac{\partial v'}{\partial r'}\right) + \frac{1}{r'^2}\frac{\partial^2 v'}{\partial \theta'^2} + \frac{\partial^2 v'}{\partial z'^2} + \frac{2}{r'^2}\frac{\partial u'}{\partial \theta'}\right) \quad (3)$$

$$\frac{\partial w'}{\partial t'} + u'\frac{\partial w'}{\partial r'} + \frac{v'}{r'}\frac{\partial w'}{\partial \theta'} + w'\frac{\partial w'}{\partial z'}$$

$$= F_{z'} - \frac{1}{\rho_{nf}}\frac{\partial p'}{\partial z'} + \frac{\mu_{nf}}{\rho_{nf}}\left(\frac{1}{r'}\frac{\partial}{\partial r'}\left(r'\frac{\partial w'}{\partial r'}\right) + \frac{1}{r'^2}\frac{\partial^2 w'}{\partial \theta'^2} + \frac{\partial^2 w'}{\partial z'^2}\right) \quad (4)$$

where F with different indices represents body forces with respect to different directions.

Diffusion equation for temperature in cylindrical co-ordinates:

$$\frac{1}{D_{nf}}\frac{\partial T'}{\partial t'} = \frac{\partial^2 T'}{\partial r'^2} + \frac{1}{r'}\frac{\partial T'}{\partial r'} + \frac{1}{r'^2}\frac{\partial^2 T'}{\partial \theta'^2} + \frac{\partial^2 T'}{\partial z'^2} + \frac{H}{k_{nf}} \quad (5)$$

where D_{nf} is the thermal diffusivity.

The governing equations (1), (2) and (3) are solved under the following assumptions:

1. Flow is considered two dimensional.
2. Flow is axisymmetric.
3. The radial and azimuthal components of fluid velocity are zero.
4. The axial and azimuthal components of temperature are zero.
5. The heat transfer is considered to take place via diffusion in the arteriole.
6. Constant heat source parameter is considered for heat generation/absorption under the effect of nanofluid flow.

The modified equations are given henceforth.

The equation of motion for peripheral layer is:

$$-\frac{\partial P'}{\partial z'} + \frac{\mu_f}{r'}\frac{\partial}{\partial r'}\left(r'\frac{\partial u'_0}{\partial r'}\right) = 0 \quad (6)$$

where μ_f is the viscosity of plasma.

No slip condition is assumed at the arteriolar wall. Hence, the boundary conditions are stated as:

$$u'_0 = 0 \text{ at } r' = R_0 \quad (7)$$

The equation of motion and heat in the presence of nanoparticles for the central region is:

$$-\frac{\partial P'}{\partial z'} + \frac{1}{r'}\frac{\partial}{\partial r'}(r'\tau_{nf}) + g(\rho\gamma)_{nf}(T'-T_0) = 0 \tag{8}$$

$$\frac{\partial^2 T'}{\partial r'^2} + \frac{1}{r'}\frac{\partial T'}{\partial r'} + \frac{H}{k_{nf}} = 0 \tag{9}$$

where T' is temperature, τ_{nf} is shear stress of nanofluid, $(\rho\gamma)_{nf}$ is thermal expansion of nanofluid and k_{nf} is nanofluid thermal conductivity in the central region of the arteriole. H is a constant heat generation or absorption parameter. T_0 is the temperature of the peripheral layer.

The velocity and shear stress are continuous at the interphase of the peripheral layer and central layer. Hence, the boundary conditions are stated as:

$$u'_0 = u'_1 \quad \text{at} \quad r' = R'_1 \tag{10}$$

$$\tau_f = \tau_{nf} \quad \text{at} \quad r' = R'_1 \tag{11}$$

The temperature is prescribed T_0 all over surface of the central region and the temperature gradient vanishes along the axis of the arteriole.

$$T' = T_0 \quad \text{at} \quad r' = R'_1 \tag{12}$$

$$\frac{\partial T'}{\partial r'} = 0 \quad \text{at} \quad r' = 0 \tag{13}$$

The equation of motion for the core region is:

$$\frac{\partial u'_c}{\partial r'} = 0 \tag{14}$$

where u'_c is velocity in the core region.

The velocity gradient vanishes along the axis of the arteriole. Hence, the boundary conditions are stated as:

$$\frac{\partial u'_1}{\partial r'} = \frac{\partial u'_c}{\partial r'} = 0 \quad \text{at} \quad r' = 0 \tag{15}$$

$$u'_c = u'_1 \quad \text{at} \quad r' = R_c \tag{16}$$

Nanofluids are described as advanced colloidal fluids obtained by the dispersion of 1-100 nm nanoparticles in standard fluids [10]. It has been shown experimentally that nanofluids have greater conductivity than base fluids. Maxwell introduced the first mathematical model to devise the thermal conductivity of nanoparticle suspensions. Maxwell's Effective Medium Theory (EMT) [27] was further developed by Hamilton and Crosser for non-spherical shaped particles.

The Hamilton-Crosser model describes the total thermal conductivity of two components in a heterogeneous mixture. It is a relation to the thermal conductivity of the pure materials, their respective compositions and the fashion in which they are scattered throughout the mixture [28]. It calculates the total thermal conductivity (k_{nf}) of the heterogeneous mixture. It includes shape factor $n = 3/\psi$ where ψ is recognized as sphericity which is termed as the ratio of the surface area of the sphere to the surface area of the real particle with equal volumes. The value of n or shape

factor for various shapes of nanoparticles [30] is listed in Table 1.

$$\frac{k_{nf}}{k_f} = \frac{k_p + (n-1)k_f + (n-1)(k_p - k_f)\phi}{k_p + (n-1)k_f - (k_p - k_f)\phi} \tag{17}$$

where k_p represents the thermal conductivity of the nanoparticles, k_f represents the thermal conductivity of blood. ϕ is the volume fraction of the nanoparticles in the blood.

According to the principle of conservation of mass of two species, the density of nanofluid [6] is expressed as

$$\rho_{nf} = (1-\phi)\rho_f + \phi\rho_p \tag{18}$$

The thermal expansion of the nanofluid $(\rho\gamma)_{nf}$ is expressed as

$$(\rho\gamma)_{nf} = (1-\phi)(\rho\gamma)_f + \phi(\rho\gamma)_p \tag{19}$$

The viscosity of the nanofluid u_{nf} [6] is expressed as

$$\mu_{nf} = \mu_f(1+\alpha\phi) \tag{20}$$

where is ρ_f the density, $(\rho\gamma)_f$ is the thermal expansion and μ_f is the viscosity of the blood. ρ_p is the nanoparticle density and $(\rho\gamma)_p$ is the nanoparticle thermal expansion. The value of α depends on the shape of the nanoparticles [19] listed in Table 1.

The non-dimensional scheme is stated as:

$$z = \frac{z'}{R_0}, \ u_0 = \frac{u_0'}{u_{avg}}, \ u_c = \frac{u_c'}{u_{avg}}, \ u_1 = \frac{u_1'}{u_{avg}}, \ P = \frac{P'}{\rho_f u_{avg}^2}, \ Re = \frac{R_0 u_{avg} \rho_f}{\mu_f},$$

$$\theta = \frac{T' - T_0}{T_1 - T_0}, \ Gr = \frac{g(\rho\gamma)_f R_0^2 (T_1 - T_0)}{u_{avg} \mu_f}, \ \beta = \frac{QR_0^2}{(T_1 - T)k_f}, \ r = \frac{r'}{R_0}, \ R_1 = \frac{R_1'}{R_0} \tag{21}$$

where u_{avg} is the average velocity, Re is the Reynolds number, Gr is the Grashof number and β is the heat source parameter.

The non-dimensional equations are stated as:

$$-Re\frac{\partial P}{\partial z} + \frac{1}{r}\frac{\partial}{\partial r}\left(r\frac{\partial u_0}{\partial r}\right) = 0 \tag{22}$$

$$-Re\frac{\partial P}{\partial z} + \frac{(1+\alpha\phi)}{r}\frac{\partial}{\partial r}\left(r\frac{\partial u_1}{\partial r}\right) + \left((1-\phi) + \phi\frac{(\rho\gamma)_p}{(\rho\gamma)_f}\right)Gr\theta = 0 \tag{23}$$

$$\frac{\partial^2\theta}{\partial r^2} + \frac{1}{r}\frac{\partial\theta}{\partial r} + \beta\left[\frac{k_p + (n-1)k_f + (n-1)(k_p - k_f)\phi}{k_p + (n-1)k_f - (k_p - k_f)\phi}\right] = 0 \tag{24}$$

$$\frac{\partial u_c}{\partial r} = 0 \tag{25}$$

The non-dimensional boundary conditions are stated as:

$$u_0 = 0 \quad \text{at} \quad r = 1 \tag{26}$$

$$u_0 = u_1 \quad \text{at} \quad r = R_1 \tag{27}$$

$$\tau_f = \tau_{nf} \quad \text{at} \quad r = R_1 \tag{28}$$

$$\frac{\partial u_1}{\partial r} = \frac{\partial u_c}{\partial r} = 0 \quad \text{at} \quad r = 0 \tag{29}$$

$$u_c = u_1 \quad \text{at} \quad r = R_c / R_0 \tag{30}$$

$$\theta = 0 \quad \text{at} \quad r = 1 \tag{31}$$

$$\frac{\partial \theta}{\partial r} = 0 \quad \text{at} \quad r = 0 \tag{32}$$

3. Solution

The solution of equations (22) to (25) using the boundary conditions (26) to (32) is obtained analytically under simplified assumptions using the method of solving partial differential equations in the following manner:

Solving equation (24) for θ in terms of r, we get

$$\theta = \beta \frac{r}{4} \left[\frac{k_p + (n-1)k_f + (n-1)(k_p - k_f)\phi}{k_p + (n-1)k_f - (k_p - k_f)\phi} \right] (1 - r) \tag{33}$$

Equation (23) is solved for u_1 using the value of θ from (33)

$$u_1 = \frac{Re}{(1+\alpha\phi)} \frac{\partial p}{\partial z} r^2 / 4 - r^2 / 2 \left(\frac{1}{2} - \frac{r}{3} \right) \beta Gr / 4 \left((1-\phi) + \phi \frac{(\rho\gamma)_p}{(\rho\gamma)_f} \right) \left[\frac{k_p + (n-1)k_f + (n-1)(k_p - k_f)\phi}{k_p + (n-1)k_f - (k_p - k_f)\phi} \right]$$

$$+ Re \frac{\partial p}{\partial z} \left(\frac{R_1^2}{4} - \frac{1}{4} - \frac{R_1^2}{4(1+\alpha\phi)} \right) + R_1^2 / 2 \left(\frac{1}{2} - \frac{R_1}{3} \right) \left(\beta Gr / 4 \left((1-\phi) + \phi \frac{(\rho\gamma)_p}{(\rho\gamma)_f} \right) \left[\frac{k_p + (n-1)k_f + (n-1)(k_p - k_f)\phi}{k_p + (n-1)k_f - (k_p - k_f)\phi} \right] \right)$$

$$+ \log R_1 \left(\left(R_1^3 / 2 \left(\beta Gr / 4 \left((1-\phi) + \phi \frac{(\rho\gamma)_p}{(\rho\gamma)_f} \right) \left[\frac{k_p + (n-1)k_f + (n-1)(k_p - k_f)\phi}{k_p + (n-1)k_f - (k_p - k_f)\phi} \right] \right) - R_1^2 / 2 - \frac{R_1^2 \alpha\phi Re}{2(1+\alpha\phi)} \frac{\partial p}{\partial z} \right) \right) \tag{34}$$

Equation (22) is solved for u_0 which is given as

$$u_0 = Re\frac{\partial p}{\partial z}\left[r^2/4 - 1/4\right]$$

$$+\log r\left(R_1^3/2\left(\beta Gr/4\left((1-\phi)+\phi\frac{(\rho\gamma)_p}{(\rho\gamma)_f}\right)\left[\frac{k_p+(n-1)k_f+(n-1)(k_p-k_f)\phi}{k_p+(n-1)k_f-(k_p-k_f)\phi}\right]\right)-R_1^2/2-\frac{R_1^2\alpha\phi Re}{2(1+\alpha\phi)}\frac{\partial p}{\partial z}\right) \quad (35)$$

Equation (25) is solved for u_c which is given as

$$u_c = \frac{Re}{(1+\alpha\phi)}\frac{\partial p}{\partial z}R_c^2/4 - R_c^2/2\left(\frac{1}{2}-\frac{R_c}{3}\right)\beta Gr/4\left((1-\phi)+\phi\frac{(\rho\gamma)_p}{(\rho\gamma)_f}\right)\left[\frac{k_p+(n-1)k_f+(n-1)(k_p-k_f)\phi}{k_p+(n-1)k_f-(k_p-k_f)\phi}\right]$$

$$+Re\frac{\partial p}{\partial z}\left(\frac{R_1^2}{4}-\frac{1}{4}-\frac{R_1^2}{4(1+\alpha\phi)}\right)+R_1^2/2\left(\frac{1}{2}-\frac{R_1}{3}\right)\left(\beta Gr/4\left((1-\phi)+\phi\frac{(\rho\gamma)_p}{(\rho\gamma)_f}\right)\left[\frac{k_p+(n-1)k_f+(n-1)(k_p-k_f)\phi}{k_p+(n-1)k_f-(k_p-k_f)\phi}\right]\right)$$

$$+\log R_1\left(\left(R_1^3/2\left(\beta Gr/4\left((1-\phi)+\phi\frac{(\rho\gamma)_p}{(\rho\gamma)_f}\right)\left[\frac{k_p+(n-1)k_f+(n-1)(k_p-k_f)\phi}{k_p+(n-1)k_f-(k_p-k_f)\phi}\right]\right)-R_1^2/2-\frac{R_1^2\alpha\phi Re}{2(1+\alpha\phi)}\frac{\partial p}{\partial z}\right)\right) \quad (36)$$

The volumetric flow rate is given as:

$$Q = Q_0 + Q_1 + Q_c \quad (37)$$

$$\text{or } Q = 2\pi\left(\int_{R_1}^1 u_0 r dr + \int_{R_c}^{R_1} u_1 r dr + \int_0^{R_c} u_c r dr\right) \quad (38)$$

The value of Q_0, Q_1 and Q_c is calculated as:

$$Q_0 = \pi Re\frac{\partial p}{\partial z}\left(\frac{R_1^2}{4}-\frac{R_1^4}{8}-\frac{1}{8}\right)+\pi\left(\frac{R_1^2}{2}-\frac{1}{2}-R_1^2\log R_1\right)$$

$$\left(\left(R_1^3/2\left(\beta Gr/4\left((1-\phi)+\phi\frac{(\rho\gamma)_p}{(\rho\gamma)_f}\right)\left[\frac{k_p+(n-1)k_f+(n-1)(k_p-k_f)\phi}{k_p+(n-1)k_f-(k_p-k_f)\phi}\right]\right)-R_1^2/2-R_1^2\alpha\phi/2(1+\alpha\phi)Re\frac{\partial p}{\partial z}\right)\right) \quad (39)$$

$$Q_1 = \pi Re\frac{\partial\rho}{\partial z}\left((R_1^4-R_c^4)/8(1+\alpha\phi)+(R_1^2-R_c^2)\left(\frac{R_1^2}{4}-\frac{1}{4}-R_1^2/4(1+\alpha\phi)\right)\right)$$

$$+\pi\left((R_1^2-R_c^2)\left(\beta Gr/4\left((1-\phi)+\phi\frac{(\rho\gamma)_p}{(\rho\gamma)_f}\right)\left[\frac{k_p+(n-1)k_f+(n-1)(k_p-k_f)\phi}{k_p+(n-1)k_f-(k_p-k_f)\phi}\right]\right)\right)$$

$$R_1^2 / 2\left(\frac{1}{2} - R_1 / 3\right) - (R_1^4 - R_c^4) / 8 + (R_1^5 - R_c^5) / 15\Bigg)$$

$$+\log R_1\left(R_1^3 / 2\left(\beta Gr / 4\left((1-\phi)+\phi\frac{(\rho\gamma)_p}{(\rho\gamma)_f}\right)\left[\frac{k_p +(n-1)k_f +(n-1)(k_p - k_f)\phi}{k_p +(n-1)k_f -(k_p - k_f)\phi}\right]\right)\right.$$

$$\left.\left.-R_1^2 / 2 - R_1^2\alpha\phi / 2(1+\alpha\phi)Re\frac{\partial p}{\partial z}\right)\pi(R_1^2 - R_c^2)\right) \qquad (40)$$

$$Q_c = \pi R_c^2\left(\frac{Re}{(1+\alpha\phi)}\frac{\partial p}{\partial z}R_c^2 / 4 - R_c^2 / 2\left(\frac{1}{2} - \frac{R_c}{3}\right)\beta Gr / 4\left((1-\phi)+\phi\frac{(\rho\gamma)_p}{(\rho\gamma)_f}\right)\right.$$

$$\left[\frac{k_p +(n-1)k_f +(n-1)(k_p - k_f)\phi}{k_p +(n-1)k_f -(k_p - k_f)\phi}\right] + Re\frac{\partial p}{\partial z}\left(\frac{R_1^2}{4} - \frac{1}{4} - \frac{R_1^2}{4(1+\alpha\phi)}\right)$$

$$+R_1^2 / 2\left(\frac{1}{2} - \frac{R_1}{3}\right)\left(\beta Gr / 4\left((1-\phi)+\phi\frac{(\rho\gamma)_p}{(\rho\gamma)_f}\right)\left[\frac{k_p +(n-1)k_f +(n-1)(k_p - k_f)\phi}{k_p +(n-1)k_f -(k_p - k_f)\phi}\right]\right)$$

$$+\log R_1\left(\left(R_1^3 / 2\left(\beta Gr / 4\left((1-\phi)+\phi\frac{(\rho\gamma)_p}{(\rho\gamma)_f}\right)\left[\frac{k_p +(n-1)k_f +(n-1)(k_p - k_f)\phi}{k_p +(n-1)k_f -(k_p - k_f)\phi}\right]\right)\right)\right)$$

$$-R_1^2 / 2 - \frac{R_1^2\alpha\phi Re}{2(1+\alpha\phi)}\frac{\partial p}{\partial z} \qquad (41)$$

4. Graphical results and discussions

A pioneering study is conducted on a three-layer model of blood flow in arterioles containing nanoparticles in the central region. The significant effect of distinct flow parameters on the nanofluid flow or nanofluid with different shapes of nanoparticles is examined in this part (Figure 2-9) with the graphs of temperature, velocity and flow rate. Table 2 and 3 lists the values used in plotting the graphs.

Figure 2 shows the graph of temperature (θ) of the nanofluid versus radial co-ordinate (r) for various shapes of nanoparticles in the blood i.e. different values of shape parameter (n). Brick-shaped nanoparticles in the blood show a maximum increase in temperature while blade-shaped nanoparticles in blood show a least rise in temperature. Brick-shaped nanoparticles have the lowest viscosity in the nanofluid, thus, maximum thermal conductivity that causes the greatest rise in temperature. Nanofluid with nanoparticles of shapes cylinders and platelets have lesser viscosity, therefore higher thermal conductivity which causes a higher rise in temperature. This is because elongated nanoparticles like cylinders and platelets exhibit greater viscosity [30]. Nanofluids with brick-shaped nanoparticles have a low viscosity in view of their shear-thinning nature with a rise in temperature which causes a maximum increase in temperature in the respective nanofluid. The result presented here agrees with the experimental results given by Timofeeva et al. [30].
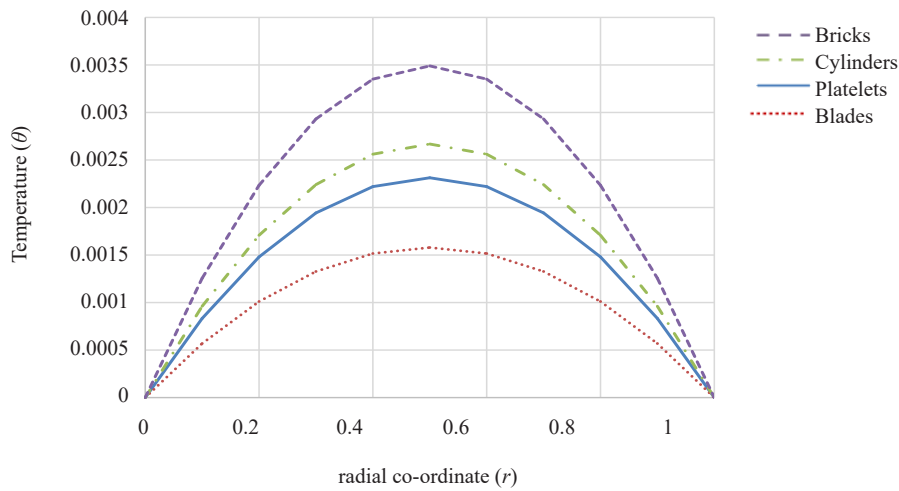
Figure 2. Temperature θ of nanofluid versus radial co-ordinate (r) for varying shapes of nanoparticles (n) ($\beta = 2.0$, $\Phi = 0.02$, $Gr = 4.0$)
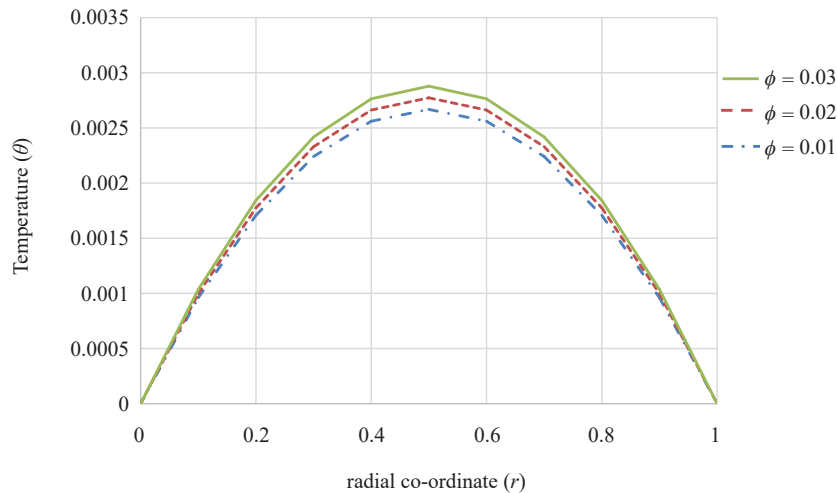
Figure 3. Temperature (θ) of nanofluid against radial co-ordinate (r) for different values of volume fraction (ϕ) of nanoparticles ($n = 4.9$, $\beta = 0.2$, $Gr = 4.0$)

Figure 3 shows the variation of temperature (θ) of nanofluid against radial co-ordinate (r) for distinct values of volume fraction (ϕ) of blade-shaped nanoparticles in the blood. It is observed from the parabolic trend that the temperature of the nanofluid rises with the increase in the volume fraction of nanoparticles in the blood. The increase in the number of nanoparticles increases the value of the volume fraction. With this increase in volume fraction, heat transfer gets dominated by conduction from the core region to the peripheral layer which causes a rise in the temperature of the nanofluid. A similar result was observed earlier by Ijaz and Nadeem [31]. This result is compatible with the physical behavior of nanoparticles in fluids.

Figure 4 shows the variation of temperature (θ) of nanofluid versus radial co-ordinate (r) for distinct values of heat source parameter (β) for blade-shaped nanoparticles. The trend of the graph is parabolic i.e. temperature is zero near the wall and maximum at the center of the axis. This is due to the fact that in arterioles hematocrit is very close to zero immediately near the wall under the influence of the wall exclusion effect while hematocrit is maximum at the axis of the wall [1]. It is seen that the nanofluid temperature rises with the rise in the value of the heat source parameter. The reason being more heat generation in the nanofluid by an increase in the effective movement of nanoparticles in the

nanofluid with the rise in heat source parameter. This result is in agreement with earlier observations given by Ijaz and Nadeem [31].
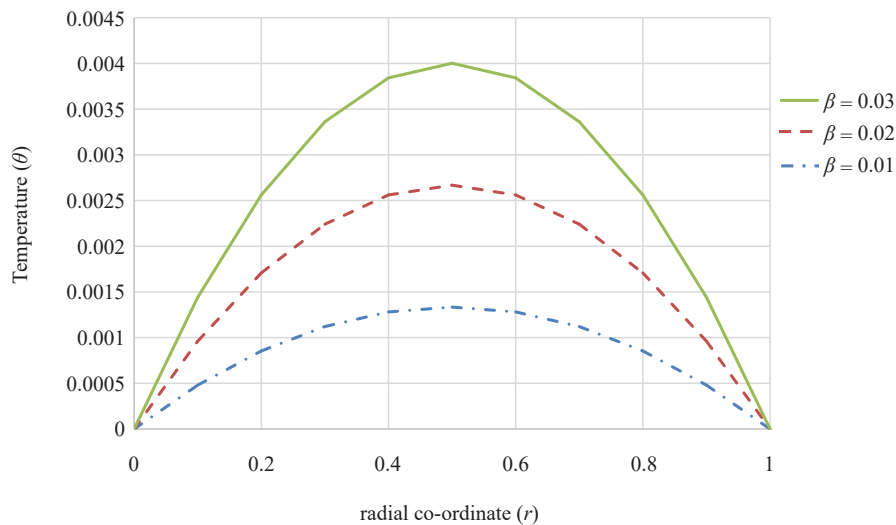
Figure 4. Temperature (θ) of nanofluid versus radial co-ordinate (r) for distinct values of heat source parameter (β) ($n = 4.9$, $\Phi = 0.02$, $Gr = 4.0$)
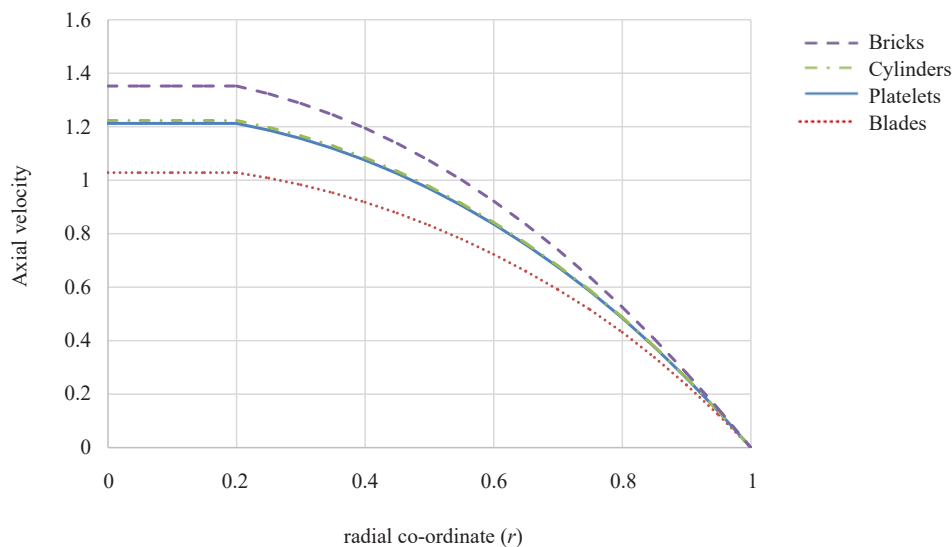
Figure 5. Axial velocity of nanofluid versus radial co-ordinate (r) for various shapes of nanoparticles (n) ($\beta = 2.0$, $\Phi = 0.02$, $Gr = 4.0$)

Figure 5 shows the graph of axial velocity of nanofluid versus radial co-ordinate (r) for varying shapes of nanoparticles in the blood i.e. different values of shape parameter (n). Brick-shaped nanoparticles in blood show the highest velocity profile while blade-shaped nanoparticles show the least velocity profile. Brick-shaped nanoparticles have the lowest viscosity in the nanofluid, thus, maximum thermal conductivity that causes the greatest rise in temperature [30]. The consequence of the shape of nanoparticles on the velocity is because of the viscosity dependence-relation of the shape of the respective nanoparticle at a given temperature [30]. Platelets and cylinders have almost the same viscosity in nanofluid due to elongated structures, thus they show an overlapping profile for velocity. Similar

results were given by Madhura et al. [28]. Blade-shaped nanoparticles show maximum viscosity while brick-shaped nanoparticles have the least viscosity.

Figure 6 depicts the variation of axial velocity of the nanofluid versus radial co-ordinate (r) using distinct values of volume fraction (ϕ) of blade-shaped nanoparticles in the blood. It is seen that the velocity decreases with rise in the value of the volume fraction of nanoparticles in the nanofluid. This is so because as the volume fraction increases, the number of nanoparticles in the blood increases, which makes the nanofluid more viscous. Identical observations were given by Timofeeva et al. [30] in their experimental study. The enhancement in viscosity causes an enhancement in the friction force which causes a reduction in velocity.
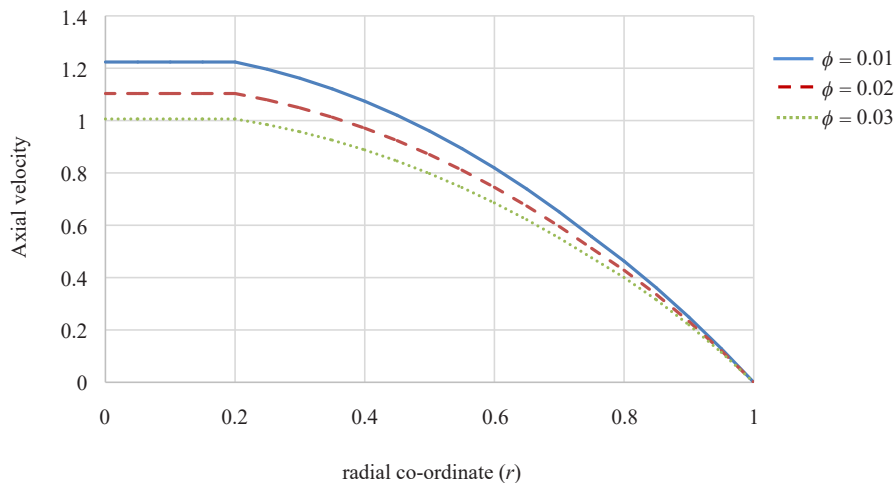
Figure 6. Axial velocity of the nanofluid versus radial co-ordinate (r) for distinct values of volume fraction (ϕ) ($\beta = 2.0$, $n = 3.9$, $\alpha = 13.5$, $Gr = 4.0$)
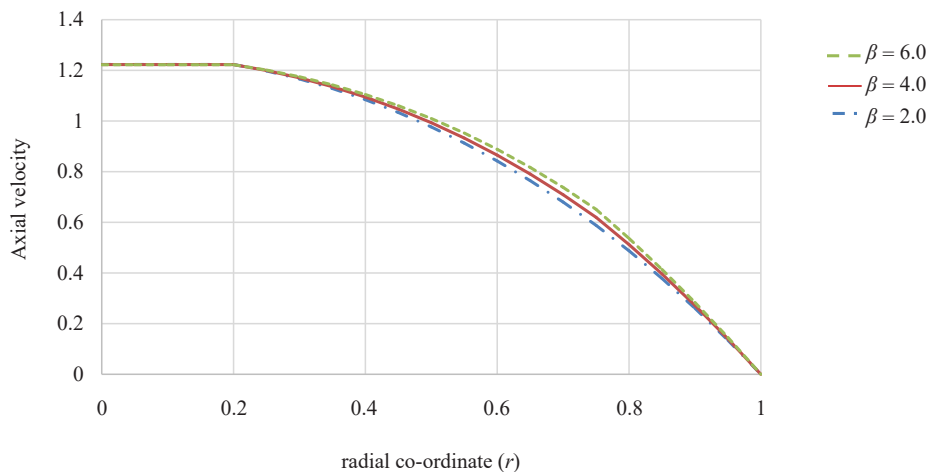
Figure 7. Axial velocity of the nanofluid versus radial co-ordinate (r) for distinct values of heat source parameter (β) ($\Phi = 0.02$, $n = 3.9$, $\alpha = 13.5$, $Gr = 4.0$)

Figure 7 exhibits the variation of axial velocity of the nanofluid versus radial co-ordinate (r) using distinguished values of heat source parameter (β) for blade-shaped nanoparticles. The enhancement in the heat source parameter causes an increase in the temperature which decreases the viscosity of nanofluids hence increasing their velocity. The calculated values of velocity in the core region for different values of heat source parameter do not have much difference

thus velocity profile can be seen overlapped in this region. An identical result was reported by Ijaz and Nadeem [31].

Figure 8 shows the variation of axial velocity of the nanofluid versus radial co-ordinate (r) for distinct values of Grashof number (Gr) for blade-shaped nanoparticles in the blood. The results show that velocity rises with the rise in the value of Grashof number. Grashof number signifies the ratio of buoyant force to the restraining forces. Buoyant forces are caused by temperature differences in the fluid and viscous forces are the restraining forces. The increase in Grashof number increases the upward buoyancy force. Therefore, the motion of nanofluids increases with increasing Grashof number because of the increase in buoyancy force. The increase in value of Grashof number reduces the viscosity of the nanofluid which thus increases the velocity. These results were also analyzed by Ijaz and Nadeem [31]. Rahbari et al. [32] and Imran et al. [33] also discussed similar observations.
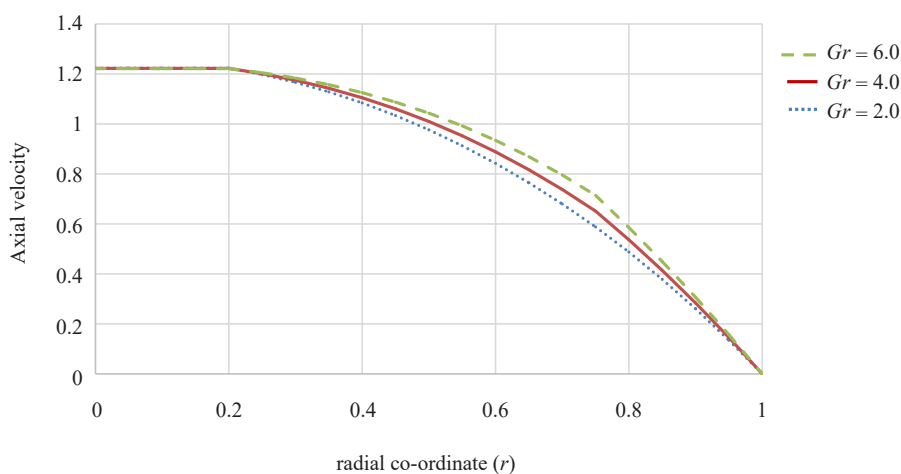
Figure 8. Axial velocity of nanofluid against radial co-ordinate (r) for distinct values of Grashof number (Gr) ($\Phi = 0.02$, $n = 3.9$, $\alpha = 13.5$, $\beta = 2.0$)
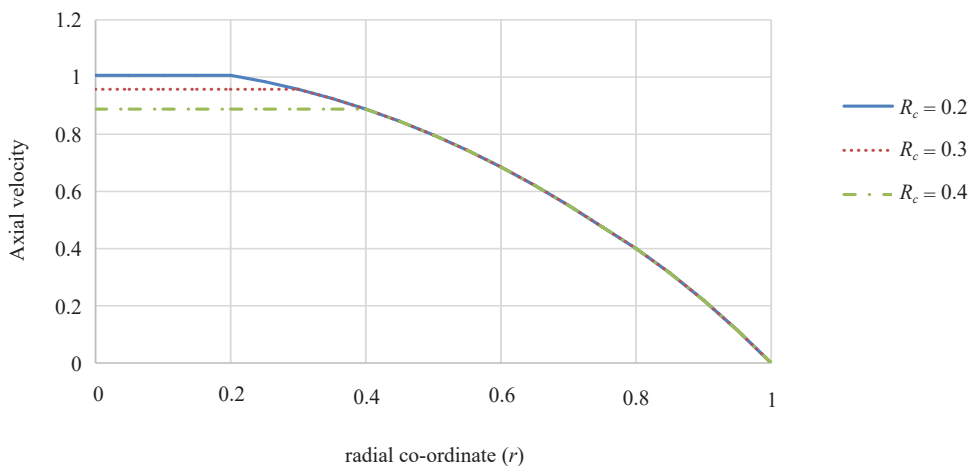
Figure 9. Axial velocity of nanofluid versus radial co-ordinate (r) for distinct values of core region R_c ($\Phi = 0.02$, $n = 3.9$, $\alpha = 13.5$, $\beta = 2.0$, $Gr = 4.0$)

Figure 9 depicts the graph of axial velocity of the nanofluid versus radial co-ordinate (r) for distinct values of core region (R_c) for blade-shaped nanoparticles in the blood. The graph depicts that the increase in the radius of the core region causes a decline in the velocity of the core region. Narrower the radius of the core region, the lesser the number

of red blood cells, the lesser the viscosity and hence the greater the velocity of the blood with nanoparticles. Similar observations were given by Bali et al. [5] and Srivastava [34].

Figure 10 shows the graph of flow rate (Q) of the nanofluid against pressure gradient ($-\partial p / \partial z$). The results show a straight-line trend for varying shapes of nanoparticles in the blood. Bali et al. [5] obtained a similar trend for flow rates. The shape factor (n) varies with the complete surface area of the nanoparticle and fluid interface. The shape factor approximately describes the ratio of the surface area of the real particle and the surface area of the sphere with the same volume [30]. Greater the value of the shape factor greater the interface. At a given temperature, nanoparticles with a higher shape factor show a lesser enhancement in flow rate because of higher viscosity [30]. The value of the shape factor is largest for blades and minimum for bricks. Thus, blades show a minimum slope and bricks show a maximum slope in the graph of flow rate against pressure gradient.
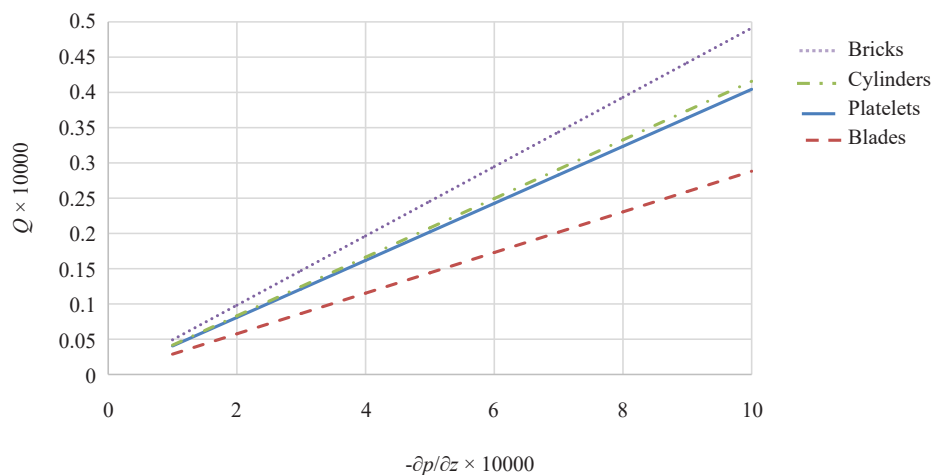
Figure 10. Flow rate (Q) against pressure gradient ($-\partial p/\partial z$)
for varying shapes of nanoparticles (n) in the blood ($\bar{\beta} = 2.0$, $\Phi = 0.02$, $Gr = 4.0$)

Axial velocity representation in graphs (Figure 5-8)
• Velocity in the core region or u_c is plotted in the region from 0 to R_c i.e. 0 to 0.2 on the radial co-ordinates.
• Velocity in the central region or u_1 is plotted in the region from R_c to R_1 i.e. 0.2 to 0.85 on the radial co-ordinates.
• Velocity in the peripheral layer or u_0 is plotted in the region from R_1 to R_0 i.e. 0.85 to 1.0 on the radial co-ordinates.

5. Conclusion

The influence of different shapes of nanoparticles is analyzed in an arteriole. Three-layer model for narrow vessels is used to model the flow of nanofluid. In the present work, we have used Hamilton and Crosser model and found that our analytical results are in agreement with the experimental results obtained by Timofeeva et al. [30]. The major findings of the analysis are summarized as follows:

• In order to develop a better understanding of physiological conditions under the influence of nanofluids, the three-layer model holds significance, which can be seen in the results obtained. The velocity trends obtained are similar to that of the Hagen-Poiseuille flow.

• The maximum increase in temperature is seen in bricks because of their shear-thinning behavior and the minimum is shown by blades. The observed trend can be stated as bricks > cylinders > platelets > blades.

• The velocity profile exhibits that maximum velocity is of bricks and minimum is of blades and the trend can be stated as bricks > cylinders ≈ platelets > blades.

• The velocity of the blood with nanoparticles increases with the enhancement in Grashof number.

• The flow rate against the pressure gradient for different shapes of nanoparticles shows a straight-line trend. The maximum slope is observed for bricks and the minimum for blades.

• Brick-shaped nanoparticles have the highest velocity in blood, thus, they will reach the diseased site as soon as possible with decreased temperature, in comparison to other shaped nanoparticles.

Over all discussions and observations show that nanoparticles with respect to parameters like shape, volume fraction, heat source parameters and Grashof number can be suitably implemented for nanoparticle drug delivery in the therapeutics of cardiovascular diseases.

Funding statement

Conflicts of interest

The authors declare that there are no conflicts of interest regarding the publication of this paper.

References

[1] Gupta BB, Nigam KM, Jaffrin MY. A three-layer semi-empirical model for flow of blood and other particulate suspensions through narrow tubes. *Journal of Biomechanical Engineering*. 1982; 104(2): 129-135.

[2] Mishra JC, Adhikary SD, Shit GC. Multiphase flow of blood through arteries with a branch capillary: A theoretical study. *Journal of Mechanics in Medicine and Biology*. 2011; 7(4): 395-417. Available from: doi: 10.1142/S021951940700239X.

[3] Srivastava VP. A theoretical model for blood flow in small vessels. *Applications and Applied Mathematics*. 2007; 2(1): 51-65.

[4] Chaturani P, Biswas D. Three-layered Couette flow of polar fluid with non-zero particle spin boundary condition at the interfaces with applications to blood flow. *Biorheology*. 1983; 20(6): 733-744. Available from: doi: 10.3233/bir-1983-20602.

[5] Bali R, Mishra S, Tandon PN. Three-layer model for blood flow in small vessels. *e-Journal of Science and Technology*. 2016; 11(1): 121-130.

[6] Debnath S, Saha AK, Roy AK. A study on solute dispersion in a three-layer blood-like liquid flowing through a rigid artery. *Periodica Polylichnica Mechanical Engineering*. 2017; 61(3): 173-183. Available from: doi: 10.3311/PPme.9378.

[7] Roy AK, Shaw S. Shear augmented microvascular solute transport with a two-phase model: Application in nano-particle assisted drug delivery. *Physcis of Fluids*. 2021; 33: 031904. Available from: doi: 10.1063/5.0035754.

[8] Qiu L, Zhu N, Feng Y, Michaelides EE, Zyla G, Jing D, et al. A review of recent advances in thermophysical properties at the nanoscale: From solid state to colloids. *Physics Reports*. 2020; 843: 1-81. Available from: doi: 10.1016/j.physrep.2019.12.001.

[9] Bali R, Prasad B, Mishra S. A review on mathematical models for nanoparticle delivery in the blood. *International Journal of Advanced Research*. 2022; 10(04): 130-146. Available from: doi: 10.21474/IJAR01/14526.

[10] Rawat SK, Upreti H, Kumar M. Comparative study of mixed convective MHD Cu-water nanofluid flow over a cone and wedge using modified Buongiorno's Model in presence of thermal radiation and chemical reaction via Cattaneo-Christov double diffusion model. *Journal of Applied and Computational Mechanics*. 2021; 7(3): 1383-1402. Available from: doi: 10.22055/JACM.2020.32143.1975.

[11] Choi SUS, Eastman JA. Enhancing thermal conductivity of fluids with nanoparticle. *Proceedings of the International Mechanical Engineering Congress and Exhibition*. 1995; 231: 99-105.

[12] Singh K, Rawat SK, Kumar M. Heat and mass transfer on squeezing unsteady MHD nanofluid flow between parallel plates with slip velocity effect. *Journal of Nanoscience*. 2016. Available from: doi: 10.1155/9708562.

[13] Simpson S, Schelfhout A, Golden C, Vafaei S. Nanofluid thermal conductivity and effective parameters. *Applied Sciences*. 2019; 9(1): 87.

[14] Yudi D, Xudong Z, Haibin S, Qiangnan H, Zijian W, Wenzhen L, et al. Application of the nano-drug delivery system in treatment of cardiovascular diseases. *Frontiers in Bioengineering & Biotechnology*. 2020; 7: 489. Available from: doi: 10.3389/fbioe.2019.00489.

[15] Shubhika K. Nanotechnology and medicine-the upside and downside. *International Journal of Drug Development and Research*. 2013; 5(1): 1-10.

[16] Goncalves I, Souza R, Coutinho G, Miranda J, Moeta A, Pereira JE, et al. Thermal conductivity of nanofluids: A review on prediction models, controversies and challenges. *Applied Sciences*. 2021; 11: 2525. Available from: doi: 10.3390/app11062525.

[17] Moghaddam HA, Ghafouri A, Khouzestani RF. Viscosity and thermal conductivity correlations for various nanofluids based on different temperature and nanoparticle diameter. *Journal of the Brazilian Society of Mechanical Sciences and Engineering*. 2021; 43: 303. Available from: doi: 10.1007/340430-021-03017-1.

[18] Rahbari A, Fakour M, Hamzehnezhad A, Vakilabadi MA, Ganji DD. Heat transfer and fluid flow of blood with nanoparticles through porous vessels in a magnetic field: A quasi-one-dimensional analytical approach. *Mathematical Biosciences*. 2017; 283: 38-47. Available from: doi: 10.1016/j.mbs.2016.11.009.

[19] Imran A, Akhtar R, Zhiyu Z, Shoaib M, Raja MAZ. Heat transfer analysis of biological nanofluid flow through ductus efferentes. *AIP Advances*. 2020; 10: 035029. Available from: doi: 10.1063/1.5135298.

[20] Shaw S, Murthy PVSN. Magnetic targeting in the impermeable micro-vessel with two-phase fluid model Non-Newtonian characteristics of blood. *Microvascular Research*. 2010; 80(2): 209-220. Available from: doi: 10.1016/j.mvr.2010.05.002.

[21] Singh SK, Kaushik SC, Tyagi VV, Tyagi SK. Experimental and computational investigation of waste heat recovery from combustion device for household purposes. *International Journal of Energy and Environmental Engineering*. 2021; 13: 353-365. Available from: doi: 10.1007/s40095-021-00430-z.

[22] Changdar S, De S. Investigation of nanoparticle as a drug carrier suspended in a blood flowing through an inclined multiple stenosed artery. *BioNanoScience*. 2017; 8: 166-178. Available from: doi: 10.1007/s12668-017-0446-7

[23] Tripathi J, Vasu B, Beg OA, Mounika BR, Gorla RSR. Numerical simulation of the transport of nanoparticles as drug carriers in hydromagnetic blood flow through a diseased artery with vessel permeability and rheological effects. *Microvascular Research*. 2022; 139: 104241. Available from: doi: 10.1016/j.mvr.2021.1042421.

[24] Moshfeghi R, Toghraie D. An analytical and statistical review of selected researches in the field of estimation of rheological behaviour of nanofluids. *Powder Technology*. 2021; 398: 117076. Available from: doi: 10.1016/j.powtec.2021.117076.

[25] Yanhua L, Yuling Zi, Mingyan M, Zihao X, Hua W. Using molecular dynamics simulations to investigate the effect of the interfacial nanolayer structure on enhancing the viscosity and thermal conductivity of nanofluids. *International Communications in Heat and Mass Transfer*. 2021; 122: 105181. Available from: doi: 10.1016/j.icheatmasstransfer.2021.105181.

[26] Maxwell JC. *A Treatise on Electricity and Magnetism*. Oxford: Clarendon Press; 1873.

[27] Hamilton RL. Thermal conductivity of heterogeneous two-component systems. *Industrial & Engineering Chemistry Fundamentals*. 1962; 187-191. Available from: doi: 10.1021/i160039005.

[28] Madhura KR, Atiwali B, Iyengar SS. Influence of nanoparticle shapes on natural convection flow with heat and mass transfer rates of nanofluids with fractional derivative. *Mathematical Methods in the Applied Sciences*. 2021; 1-17. Available from: doi: 10.1002/mma.7404.

[29] Bird RB, Stewart WE, Lightfoot EN. *Transport Phenomeon*.

[30] Devaki P, Venkateshwarlu B, Sreenadh SSS. MHD peristaltic flow of a nanofluid in a constricted artery for different shapes of nanosized particles. *Non-linear Engineering*. 2020; 9: 51-59.

[31] Pak BC, Cho YI. Hydrodynamic and heat transfer study of dispersed fluids with submicron metallic oxide particles. *Exp Heat Transfer*.1998; 11: 151-170. Available from: doi: 10.1080/08916159808946559.

[32] Batchelor GK. The effect of Brownian motion on the bulk stress in a suspension of spherical particles. *Journal of Fluid Mechanics*.1977; 83: 97-117. Available from: doi: 10.1017/s0022112077001062.

[33] Ijaz S, Nadeem S. Examination of nanoparticles as a drug carrier on blood flow through a catheterized composite stenosed artery with permeable walls. *Computer Methods and Programs in Biomedicine*. 2016; 133:83-94. Available from: doi: 10.1016/j.cmpb.2016.05.004.

[34] Timofeeva EV, Routbort JL, Singh D. Particle shape effects on thermophysical properties of alumina nanofluids. *Journal of Applied Physics*. 2009; 106: 014304. Available from: doi: 10.1063/1.3155999.

Appendix

Table 1. List of shape of nanoparticles and their shape parameter

Shapes of nanoparticles	n (shape factor)	α (shape parameter)
Platelets	5.7	37.1
Blades	8.6	14.6
Cylinders	4.9	13.5
Bricks	3.7	1.9

Source: Timofeeva et al. [30]

Table 2. Thermophysical values for blood

Thermophysical values for blood	
C_p (J/KgK) (Specific heat capacity of blood)	3594
ρ (Kg/m^3) (density of blood)	1063
k (W/mK) (thermal conductivity of blood)	0.492
γ (1/K) (thermal expansion of blood)	0.18×10^{-5}

Source: Ijaz and Nadeem [31]

Table 3. Thermophysical values for nanoparticles

Thermophysical values for nanoparticles	
C_p (J/KgK) (Specific heat capacity of copper nanoparticle)	385
ρ (Kg/m^3) (density of copper nanoparticle)	8933
k (W/mK) (thermal conductivity of copper nanoparticle)	400
γ (1/K) (thermal expansion of copper nanoparticle)	1.67×10^{-5}

Source: Ijaz and Nadeem [31]